

Adapting the AAPP microwave tests for EPS-SG

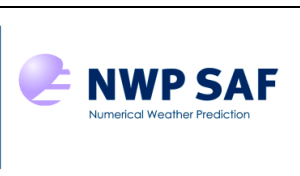
This documentation was developed within the context of the EUMETSAT Satellite Application Facility on Numerical Weather Prediction (NWP SAF), under the Cooperation Agreement dated 7 September 2021, between EUMETSAT and the Met Office, UK, by one or more partners within the NWP SAF. The partners in the NWP SAF are the Met Office, ECMWF, DWD and Météo France.

COPYRIGHT 2022, EUMETSAT, ALL RIGHTS RESERVED.

Change record			
Version	Date	Author / changed by	Remarks
1.0	23/05/2022	N C Atkinson	

Table of Contents

1.	INTRODUCTION	3
2.	TESTS IMPLEMENTED IN AAPP V8	3
3.	DIFFERENCES BETWEEN INSTRUMENTS	4
4.	SCATTERING TESTS IN AAPP	5
4.1	General approach.....	5
4.2	89 GHz test.....	5
4.3	Cirrus test – 183±7 GHz.....	8
4.4	An alternative cirrus test for MWS – 229 GHz	9
4.5	Surface and cloud liquid water test: 23.8, 31.4 and 50.3 GHz.....	12
4.6	Bennartz test	15
4.7	Redundant tests	15
5.	CONCLUSIONS	16
6.	REFERENCES	16

		<h1>Adapting the AAPP microwave tests for EPS- SG</h1>	Doc ID :NWPSAF- MO-TR-040 Version : 1.0 Date : 23/05/2022
--	--	--	---

1. INTRODUCTION

The ATOVS and AVHRR Pre-processor (AAPP) implements several microwave-based tests for cloud and precipitation. The origins of some of them date back to the 1990s, and the derivation of the coefficients was unclear in the AAPP documents. The tests were originally designed to work with AMSU-A and AMSU-B; they have since been used for MHS and ATMS, but have not explicitly taken account of changes in channel characteristics.

For the MicroWave Sounder (MWS) on EPS-SG, it is appropriate to review these microwave tests, and to decide which will be retained. Furthermore, new tests may be created to make use of the new channels that will be present in MWS.

2. TESTS IMPLEMENTED IN AAPP V8

AAPP for NOAA POES and EPS contains the following tests:

1. Scattering test: predict 89 GHz from linear combination of 23.8, 31.4 and 50.3 GHz. A scattering index (difference between predicted 89 GHz and measurement) is written to the level 1d file. The linear coefficients are scan-angle dependent (cubic polynomial in $1-\sec(z)$, where z is the zenith angle of the satellite as viewed from earth).
2. Cirrus test: predict 183 ± 7 GHz from linear combination of 23.8, 89 and 150 (AMSU-B) or 157 (MHS). A cirrus index is written to the level 1d file. The linear coefficients are scan-angle dependent (cubic polynomial in $1-\sec(z)$).
3. Surface test: identifies 8 surface types by minimising, for each spot, a cost function that uses 23.8, 31.4 and 50.3 GHz. The cost function is $(\mathbf{T}-\mathbf{T}_m)^T \mathbf{C} (\mathbf{T}-\mathbf{T}_m)$ where \mathbf{T} are the measured brightness temperatures (column vector) for the three channels and \mathbf{T}_m are the mean BTs (1 value per channel for each surface type, at 5 different zenith angles). \mathbf{C} is a covariance matrix (one matrix for each surface type, at 5 different zenith angles). This test is done on all spots; the value of the minimum of the cost function provides an indicator of the presence of cloud.
4. NWC SAF (Bennartz) test. See Bennartz et al. (2002). The index is:
 - Ocean: $(T_{89} - T_{150}) - (ave_back_sea + 0.11 z)$ where ave_back_sea is the mean of $T_{89} - T_{150} - 0.11 z$ taken over a rather large number of neighbouring sea pixels, and z is the satellite zenith angle
 - AMSU-A and MHS are over land: $(T_{23} - T_{150}) - (-1.7428 + 0.0776 z)$,
 - MHS is over land but AMSU-A is mixed: $(T_{89} - T_{150}) - (0.158 + 0.0163 z)$
 - Coast: Linear combination of the above, depending on land fraction.
5. Grody light rainfall (stated as being “redundant” in the AAPP documentation). Flag as rain if $38.0 + 0.880 T_2 > T_1$ (where T_2 is brightness temperature of channel 2 and T_1 is channel 1)
6. Crosby, Ferraro, Wu (stated as being “redundant” in the AAPP documentation). Probability of precipitation = $1/(1+\exp(-f))$ where $f = 10.5 + 0.184 T_1 - 0.221 T_2$

The tests were originally formulated to work with AMSU-A and AMSU-B. They have later been used for AMSU-A and MHS, and for ATMS, with unchanged coefficients, i.e. not optimal. See English et al. (1997).

3. DIFFERENCES BETWEEN INSTRUMENTS

The main differences between instruments are as follows:

- 23.8 GHz (channel 1) and 31.4 GHz (channel 2): QV for heritage instruments, QH for MWS
- AMSU-B has 150 GHz, MHS 157 GHz, ATMS and MWS 165.5 GHz (channel 18 for MWS)
- AMSU-B, ATMS and MWS have 183.31 ± 7 , MHS has 191.31 GHz (channel 19 for MWS)
- MWS channel 24 at 229 GHz is new.
- MWS 50 to 57 GHz channels (3-16) are nominally QH (like ATMS) but can be QV (like AMSU 3 & 4) if the backup receiver is activated.

For more detail, see Table 4 in the MWS Science Plan (MWS Science Advisory Group, 2019). The change in polarisation of channel 1 has a marked effect on the BTs, see *Figure 1*.

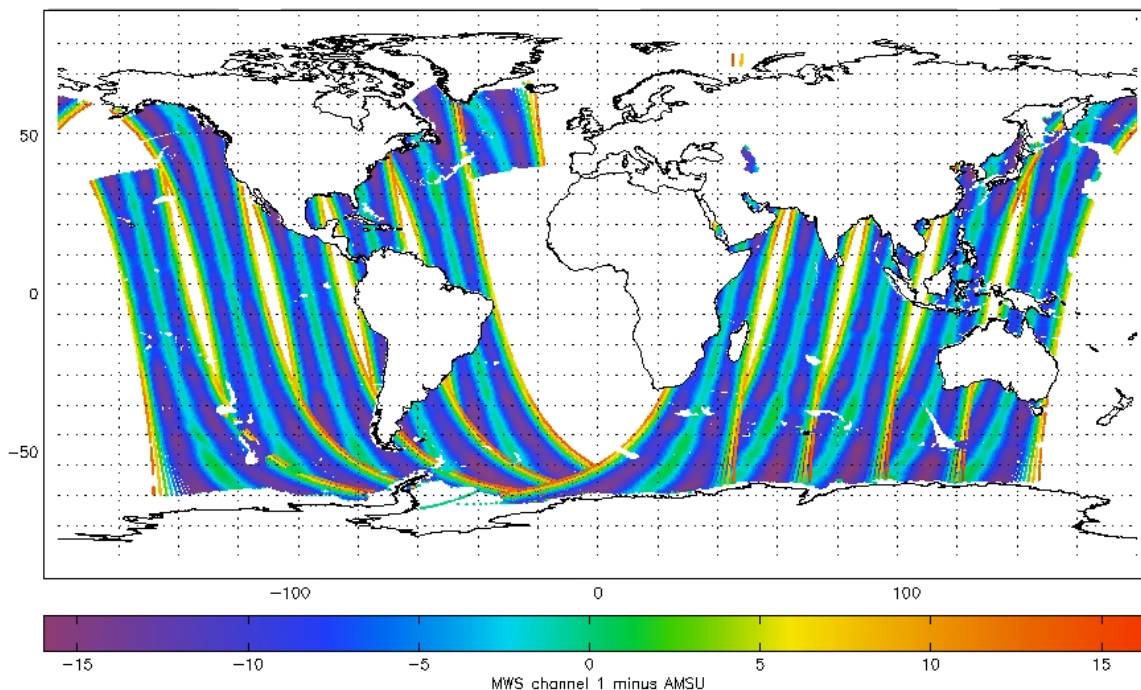


Figure 1 Effect of 23.8 GHz polarisation change in MWS, compared with AMSU-A, over ocean. The units are brightness temperature (K).

Differences between instruments can be quantified by using the following approach:

- Get NWP fields from the Met Office Unified Model (UM) for a particular model cycle (20210316 0000 was used to generate Figure 1)
- Use NOAA-18 and NOAA-19 data for AMSU, MHS and HIRS to generate HIRS 1d files (AAPP)
- Generate files containing latitude, longitude, surface height, land fraction and satellite zenith angle for Radiance Simulator input
- Run the Radiance Simulator for MWS, AMSU, MHS and ATMS. No scattering.
- Compare outputs for the different instruments. To select ocean regions, use the condition: RTTOV surface type = 0, AMSU surface type = 5, simulated channel 1 BT between 0 and 240.

4. SCATTERING TESTS IN AAPP

4.1 General approach

To predict the BT of a channel m , from channels i, j, k , AAPP uses the equation

$$\widetilde{T}_m = (1, T_i, T_j, T_k) \mathbf{M} \begin{pmatrix} 1 \\ x \\ x^2 \\ x^3 \end{pmatrix}$$

Where the tilde indicates a prediction, x is $1-\sec(z)$ where z is the zenith angle of the satellite as viewed from earth, and \mathbf{M} is a 4x4 matrix of coefficients – the columns provide zenith angle dependence and the rows provide a linear combination of the channels (the first row is a constant term).

The scattering index is then $\widetilde{T}_m - T_m$ (normally positive because scattering depresses the observed BTs).

The coefficients of \mathbf{M} can be determined from a least-squares regression. We define the dependent variable \mathbf{X} to be a matrix with *nobs* rows and 16 columns: the columns are given by 1, $x, x^2, x^3, \mathbf{T}_i, x\mathbf{T}_i, x^2\mathbf{T}_i, x^3\mathbf{T}_i, \mathbf{T}_j, x\mathbf{T}_j, x^2\mathbf{T}_j, x^3\mathbf{T}_j, \mathbf{T}_k, x\mathbf{T}_k, x^2\mathbf{T}_k, x^3\mathbf{T}_k$. The independent variable \mathbf{Y} is a vector \mathbf{T}_m , with *nobs* rows. The regression coefficients¹ are then given by

$$\text{Coefs} = (\mathbf{X}^T \mathbf{X})^{-1} (\mathbf{X}^T \mathbf{Y})$$

Note that $\mathbf{X}^T \mathbf{X}$ is a 16x16 matrix that can be inverted with, for example, LAPACK's DGETRI routine (a Fortran interface is available in the NWP SAF IRSP package).

4.2 89 GHz test

The test uses MWS channels 1, 2, 3 and 17 (23.8, 31.4, 50.3 and 89 GHz respectively).

The derived coefficients for MWS are as follows:

49.264698	436.959626	-1547.590130	1086.714673	!constant
0.823040	-0.236124	-0.613408	0.920523	!T1 (23.8 GHz)
-0.083713	-0.248160	0.511979	-0.426125	!T2 (31.4 GHz)
0.218186	-1.271136	6.032860	-4.673144	!T3 (50.3 GHz)

These can be compared with the operational coefficients used in AAPP (derived from AMSU-A):

-179.58800000	-11.82838500	-79.47264000	7.77974570	!constant
0.55091080	-0.79630378	0.82639551	-0.25387738	!T1 (23.8 GHz)
-0.24632506	0.70550387	-0.78458517	0.26119687	!T2 (31.4 GHz)
1.61315530	-0.09248847	0.41939181	-0.05278192	!T3 (50.3 GHz)

¹ https://en.wikipedia.org/wiki/Linear_regression#Least-squares_estimation_and_related_techniques

The MWS coefficients are rather different from those used in AAPP (e.g. much stronger scan dependence in the constant term) but the overall scattering signal appears reasonable (Figure 2). Remember that the scattering code in RTTOV is *not* used, therefore we would not expect any strong features to be visible. The standard deviation is 1.61K.

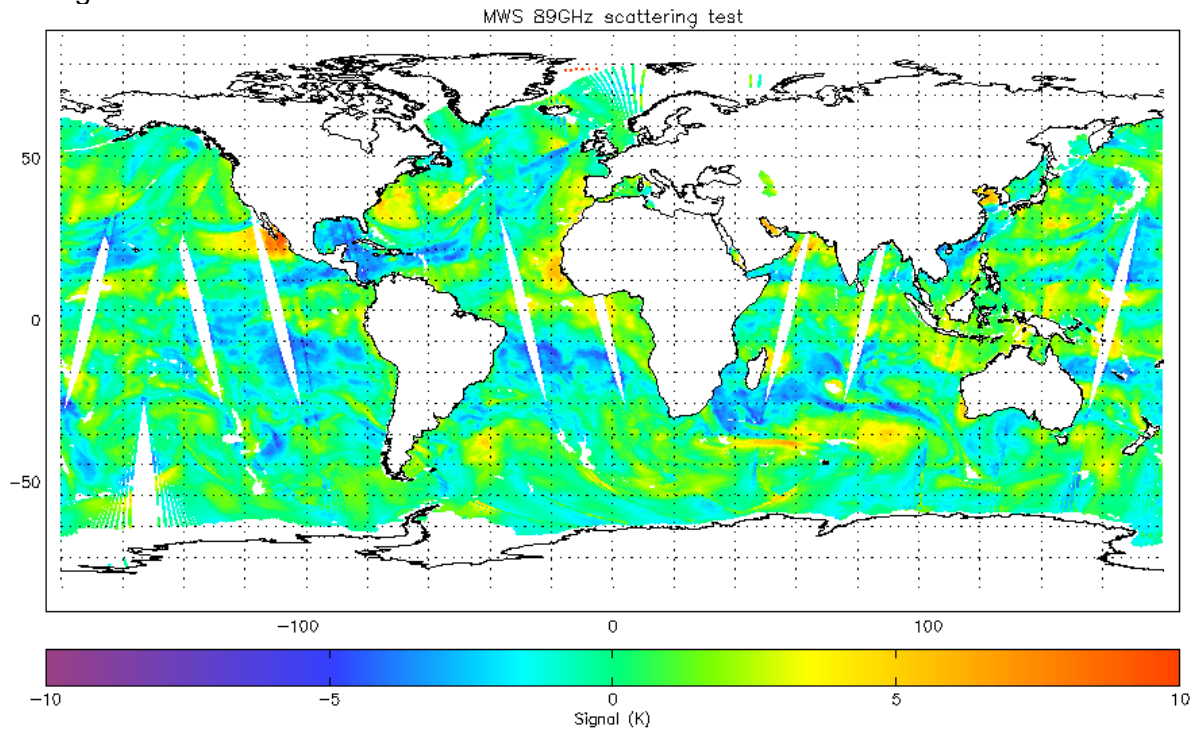


Figure 2: MWS 89 GHz scattering signal, derived from multiple linear regression from simulated data with RTTOV scattering code turned off

It is interesting to compare this with the AMSU-A 89 GHz scattering signal, again using the RTTOV simulation. This has a standard deviation of 3.05 K and is shown in Figure 3. It appears that the operational coefficients are not optimal, particularly at edge of scan and in the polar regions. It is not known in detail how they were originally derived; the code was developed in 1995.

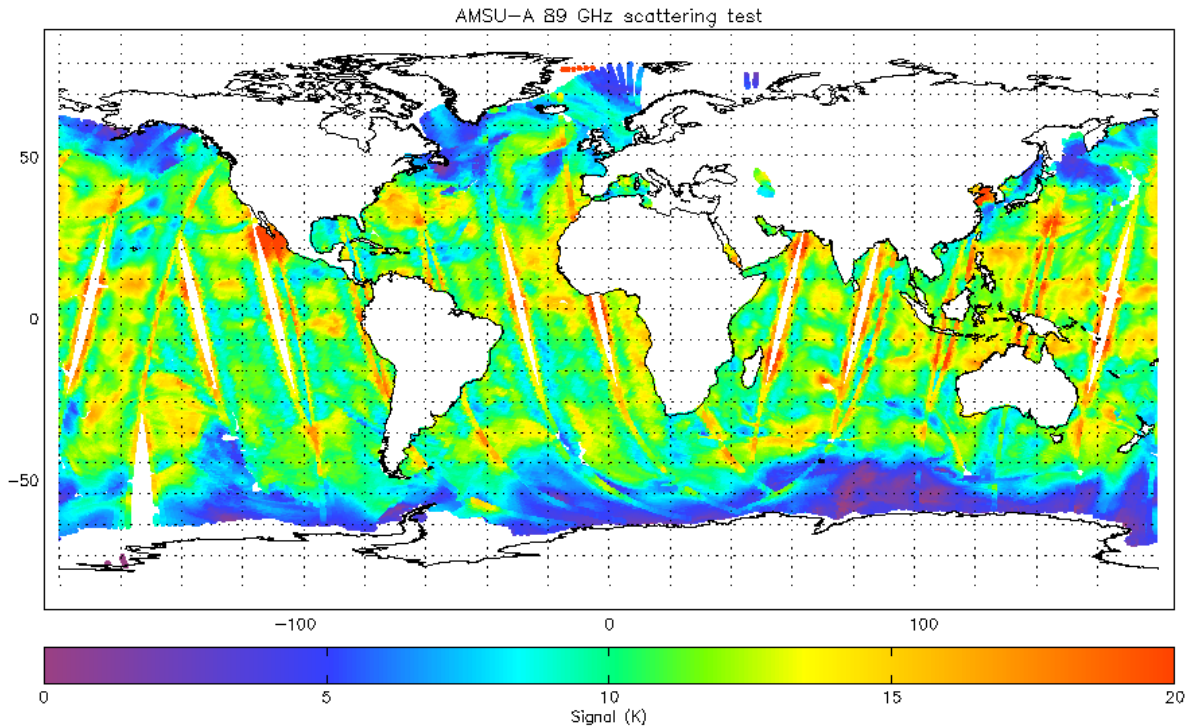


Figure 3: AMSU-A 89 GHz scattering signal, using operational AAPP coefficients

It is also informative to plot the AMSU-A scattering signal from real observations (i.e. plot the values in the ATOVS 1d file). See Figure 4. Note the scale is much wider in order to accommodate the actual scattering from clouds. When using this signal, normally a threshold test would be applied (at least 10K) in order to select cloudy regions.

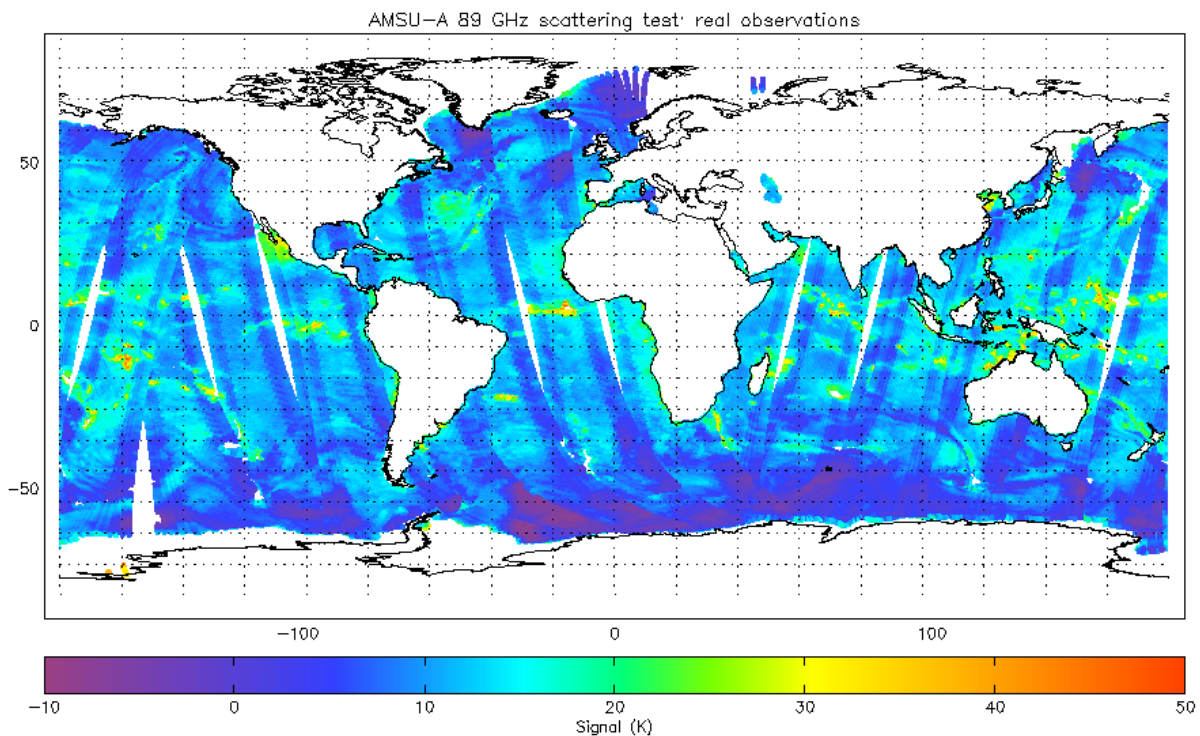


Figure 4: AMSU-A 89 GHz scattering signal extracted from AAPP level 1d files (i.e. real observations)

4.3 Cirrus test – 183±7 GHz

This test uses MWS channels 1, 17, 18 and 19 (23.8, 89, 166 and 183±7 GHz respectively).

In the same way as for the 89 GHz test, new coefficients were derived for MWS:

112.040	-192.832	309.806	-136.503	!Constant
-0.638799	-0.466943	0.386144	0.199458	!T1 (23.8 GHz)
0.343504	2.03628	-2.64216	0.734204	!T17 (89 GHz)
0.710899	-0.878897	1.27904	-0.490630	!T18 (166 GHz)

Compare the operational coefficients for AMSU-B:

135.30490000	-59.81625200	115.69066000	-44.494969	!constant
-0.34373657	0.31460922	-0.11384763	0.014299787	!T1 (23.8 GHz)
-0.27077267	0.34128134	-0.22295688	0.032319580	!T17 (89 GHz)
0.96972705	-0.25353240	-0.23358423	0.16365490	!T18 (166 GHz)

The cirrus index is plotted in Figure 5. Its standard deviation is 2.9K.

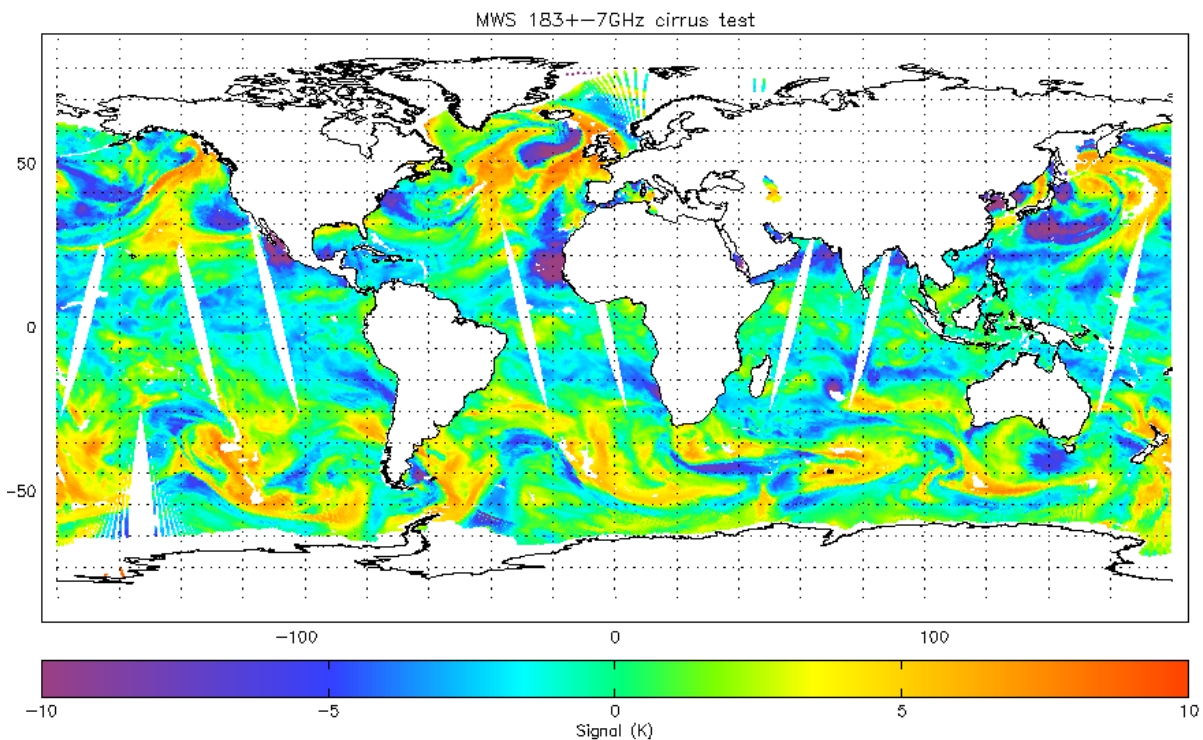


Figure 5: MWS 183±7 GHz cirrus signal, derived from multiple linear regression from simulated data with RTTOV scattering code turned off

We can also run RadSim with microwave scattering turned on in RTTOV, to simulate more closely the actual MWS signals. See Figure 6, and the corresponding Himawari-8 image in Figure 7. Although there are similarities between the scattering signal and the IR imagery, there are also differences, for example the area of strong scattering around 40N, 150E is not very prominent in the imagery.

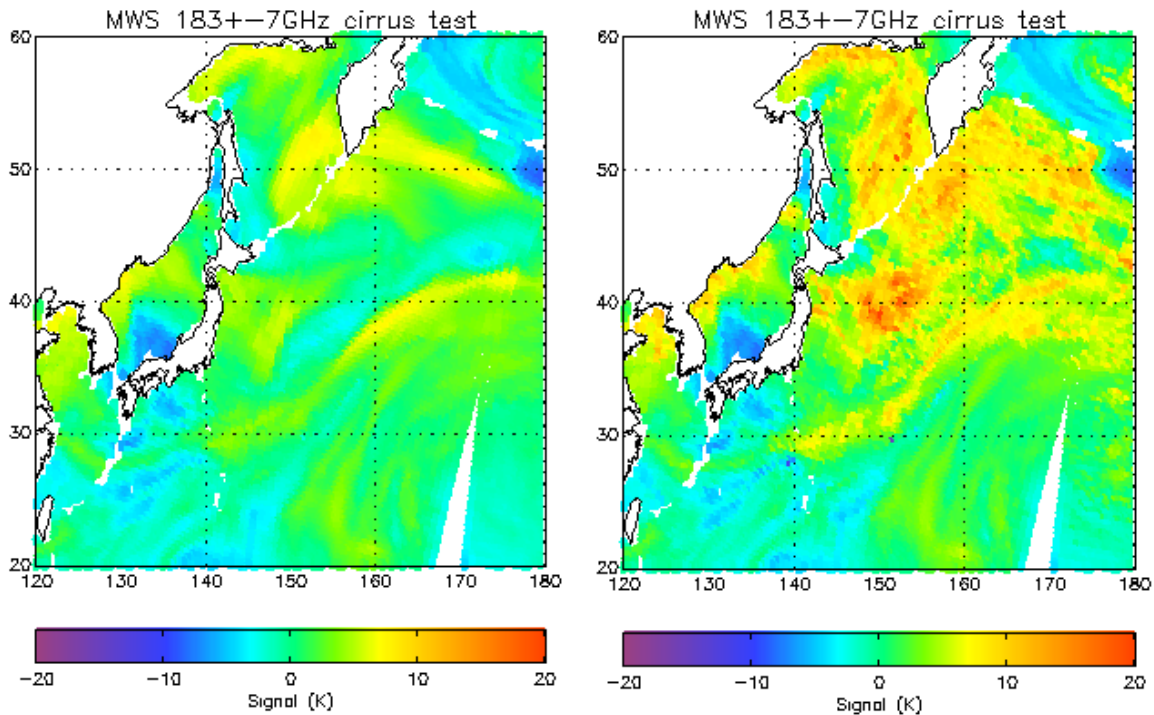


Figure 6: Cirrus test signals over SE Asia for 20210601. Left: without RTTOV-SCATT, right: with RTTOV-SCATT turned on.

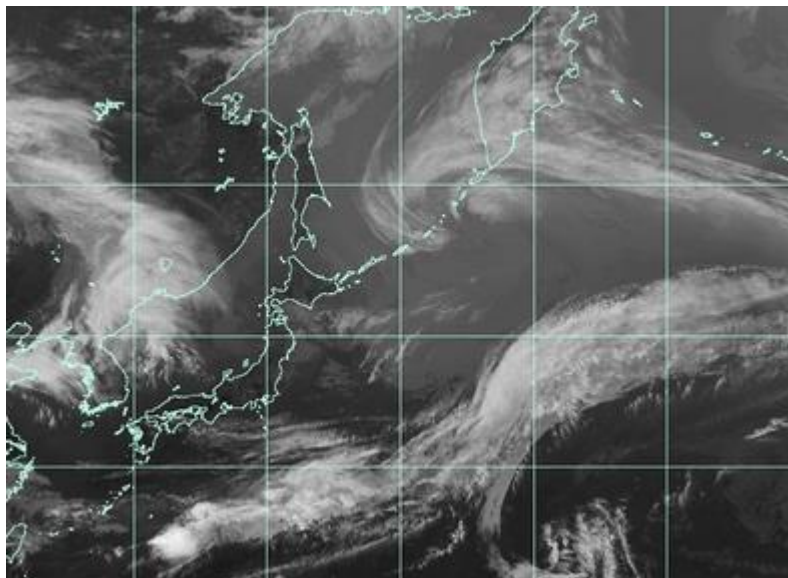


Figure 7: Himawari-8 IR 10.45 micron image at 00:00 on 1st June 2021

4.4 An alternative cirrus test for MWS – 229 GHz

An ice cloud signal that makes use of 229 GHz should be much more sensitive than one that is based on 183 ± 7 , because scattering from small ice particles increases strongly with frequency. From inspection of the simulated BTs in the clear-sky case, it was apparent that there was a strong correlation between the 166 and 229 GHz channels, stronger than for other channels. See Figure 8.

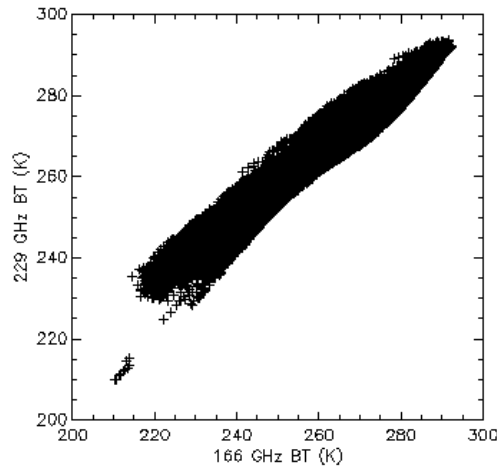


Figure 8: 166 and 229 GHz compared over sea

As a first attempt at a regression, the following coefficients were derived using these two channels, valid over sea:

```
67.229234      191.726336      -483.187476      260.834865      !constant
0.765057       -0.693036        1.715578        -0.921828      !T18 (166 GHz)
```

This gave a standard deviation of 2.2K in the difference signal, which is a little smaller than for the 183 GHz test.

Although this seems promising, it was realised that by including firstly 183±7 and secondly 89 GHz it is possible to make this test work over land also.

Coefficients for predicting 229 using two channels (166 and 183), over all surfaces, are:

```
-16.540761     -43.751113      106.705846      -53.237338      !constant
0.593588       -0.776952       2.045584        -1.124944      !T18 (166 GHz)
0.475302       0.957755        -2.486156        1.345057      !T19 (183±7 GHz)
```

with a resulting standard deviation in the signal of 1.3K

While by adding a third channel (89 GHz), we get:

```
-6.664388     -44.779022      115.411012      -64.851475      !constant
-0.052131     -0.072952       0.169709        -0.072948      !T17 (89 GHz)
0.693303      -0.767179       2.113344        -1.234298      !T18 (166 GHz)
0.385593      1.025646        -2.757663        1.573634      !T19 (183±7 GHz)
```

with a standard deviation of 1.0 K.

The cirrus index for the 3-channel regression is plotted in Figure 9. *It is recommended that this index be included in AAPP for EPS-SG.*

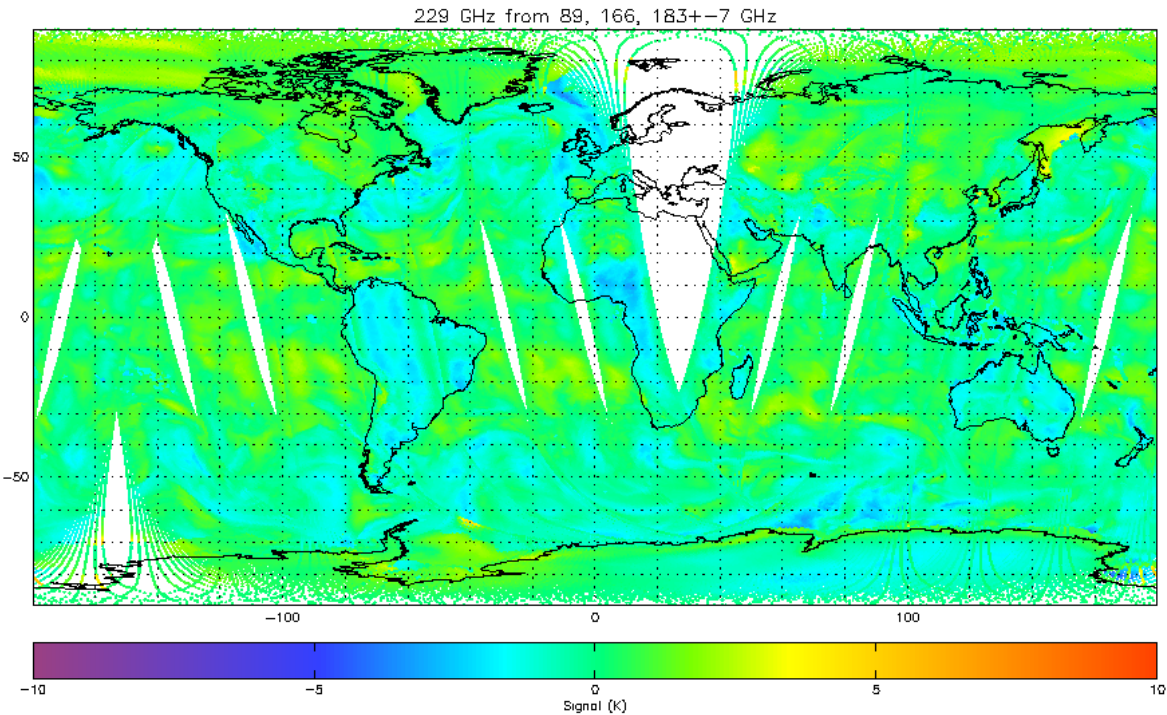


Figure 9: MWS 229 GHz cirrus signal, using 89, 166 and 183±7 as predictors.

To improve the estimate of the coefficients, the exercise was repeated using a different day, 20210601, to give a mean of the two runs:

-5.64158	-34.8024	94.7094	-54.9163	!constant
-0.0487565	-0.0544070	0.126709	-0.0497890	!T17 (89 GHz)
0.692170	-0.767554	2.13865	-1.25744	!T18 (166 GHz)
0.380185	0.971491	-2.66633	1.53854	!T19 (183±7 GHz)

Visually, it was found that there is only a slight difference between the original coefs and the new ones.

We can also run RadSim with microwave scattering turned on in RTTOV, to simulate more closely the actual MWS signals. See Figure 10. It appears that a reasonable scattering threshold is 5K. It is interesting to note that Figure 10 is emphasising different features to Figure 6 (based on 183±7).

The corresponding Himawari-8 image is repeated in Figure 11. This seems to correspond more closely to the 229 GHz product than to the 183 GHz product. A future study could perhaps compare the products with precipitation from weather radar.

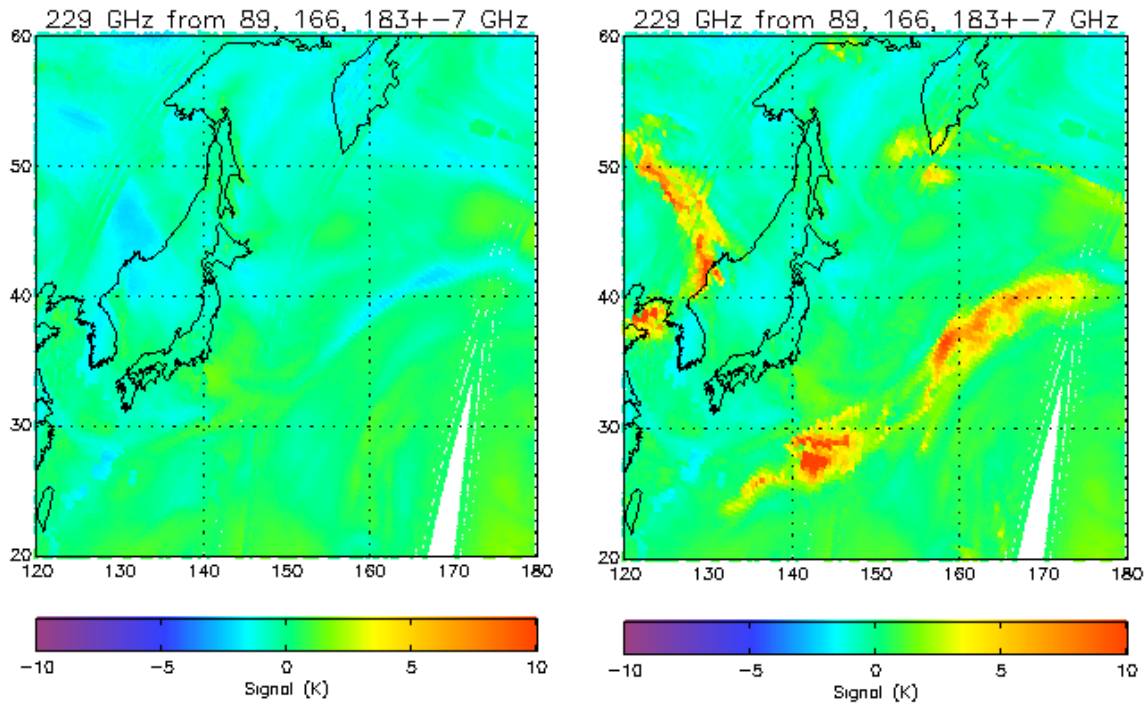


Figure 10: 229 GHz signals over SE Asia for 20210601. Left: without RTTOV-SCATT, right: with RTTOV-SCATT turned on.

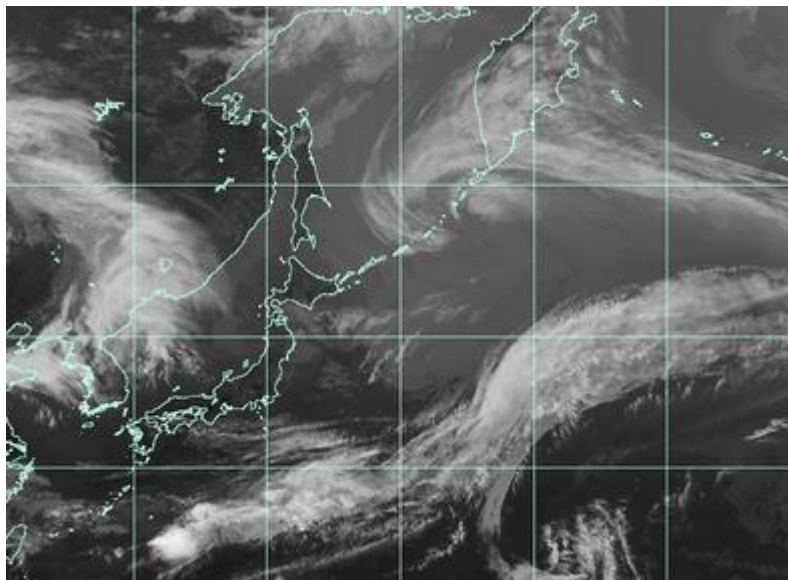


Figure 11: As Figure 7. Image repeated for ease of comparison with microwave.

4.5 Surface and cloud liquid water test: 23.8, 31.4 and 50.3 GHz

The surface test works by looking for the surface type that minimises a cost function

$$J = (T_1 - \bar{T}_1, T_2 - \bar{T}_2, T_3 - \bar{T}_3) \mathbf{C}^{-1} \begin{pmatrix} T_1 - \bar{T}_1 \\ T_2 - \bar{T}_2 \\ T_3 - \bar{T}_3 \end{pmatrix}$$

where \mathbf{C} is a 3x3 covariance matrix. Values of \mathbf{C} , \bar{T}_1 , \bar{T}_2 and \bar{T}_3 are provided for 5 different zenith angles ($\sec(z) = 1.0, 1.25, 1.5, 1.75, 2.0$), and they are interpolated for each observation. Matrices are provided for 8 surface types, and a ninth (desert) is deduced afterwards from a test of channel 1 BT. The types are shown in Table 1. The principles for distinguishing the various types, based on emissivity characteristics (including variation with frequency) are given in Grody (1988).

Table 1: Microwave surface types in AAPP

Type number	Description
1	Bare young ice (i.e. new ice, no snow)
2	Dry land (i.e. dry with or without significant vegetation)
3	Dry snow (i.e. snow with water less than 2%, over land)
4	Multi-year ice (i.e. old ice with snow [assumed dry] cover)
5	Sea (i.e. open water, no islands, ice-free, WS=0 to 14m/s)
6	Wet forest (i.e. established forest with wet canopy)
7	Wet land (i.e. non-forested land with a wet surface)
8	Wet snow (i.e. snow with water content > 2%, over land or ice)
9	Desert

The value of the cost function, after surface type identification, gives an indication of cloud liquid water. As stated in English (1997): *In simple terms, AMSU-A channel 1 is sensitive to total water vapour, channel 2 cloud liquid water and channel 3 absorber temperature. Because the covariance due to water vapour and temperature variations is large in channels 1 and 3, changes in the atmospheric profile have little impact on the cost, \mathbf{J} . However, the introduction of liquid water, which increases channel 2 out of proportion, leads to a very rapid rise in cost. This test is sensitive enough to the presence of cloud liquid water to detect cloud amounts below 100 gm^{-2} .*

Note that matrix \mathbf{C} is symmetric and its terms are all positive. \mathbf{C}^{-1} is also symmetric but can have negative off-diagonal terms.

It is not known exactly what database was used to establish this test. The AAPP Scientific Description states: “Mean brightness temperatures and BT covariance matrices have been calculated (with a radiative transfer model) for the 20 AMSU channels for different surface types, with no cloud liquid water.” Moreover, the document also says, “the coefficients are not well developed and its results are currently not very meaningful.”

It is likely that the FASTEM land/sea-ice component was used. This is configurable via 5 input parameters to represent different surface types for MW emissivities (the “Grody parameters”). This code is still available in the current FASTEM (part of RTTOV), but it is considered to be deprecated (J. Hocking, pers. comm.).

Different centres would be expected to have different uses for the AAPP surface test output. At the Met Office, it is used (i) to improve the profile surface type and to set “mismatch” flags if the AAPP surface type differs from the model type, and (ii) to set an appropriate emissivity over sea ice (B. Candy, pers. comm). The Met Office requirement is for the AAPP test to distinguish between (i) sea, (ii) multi-year ice and (iii) other surfaces.

Figure 12 shows the AMSU surface type for NOAA-18 and NOAA-19 observations for the 00Z cycle on 16th March 2021. We can see that sea areas are correctly identified as type 5. Land areas are mostly classified as dry land (type 2) or wet land (type 7); it is not obvious whether there is any skill in distinguishing them. The main areas of wet forest (type 6) are over polar sea-ice – which is

not realistic! There are some areas classified as multi-year ice (type 4) in the Arctic, but also some areas in central Asia which are more likely to be desert. Almost no areas are actually classified as desert.

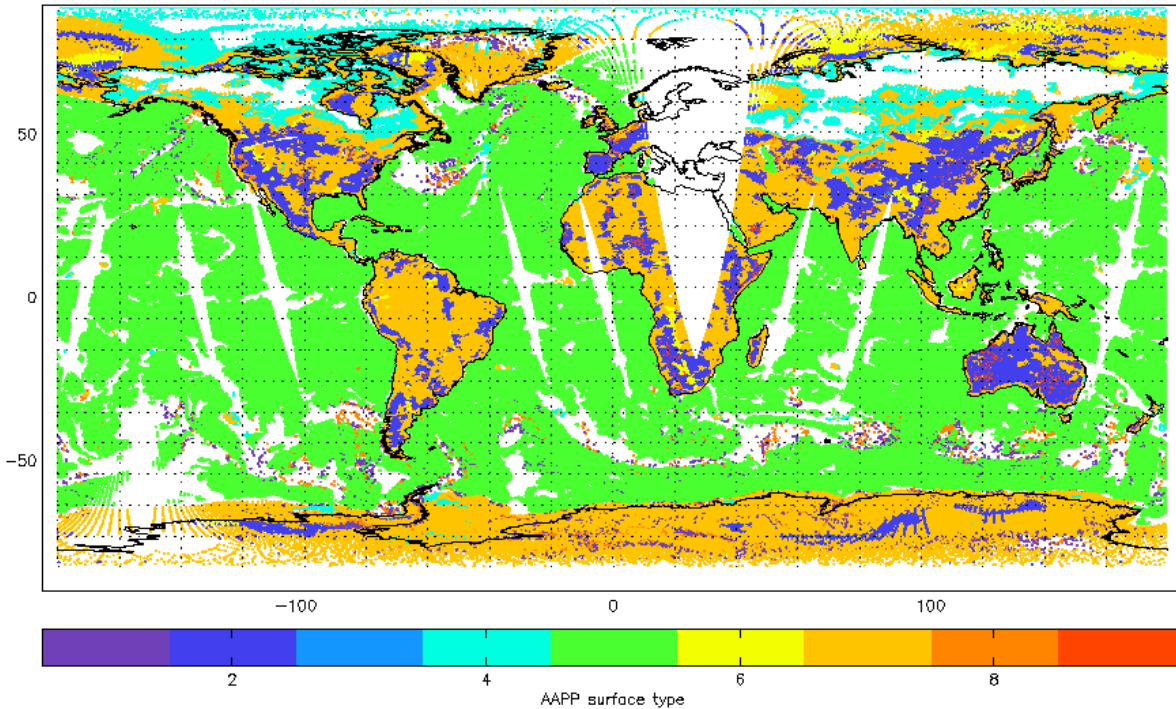


Figure 12: AMSU surface type from AAPP for samples with surface cost < 10K

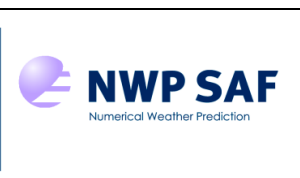
The simplest way to adapt this surface test for EPS-SG would be to take the sea category only (since that is the one most affected by the channel 1 & 2 polarisation change) and simply to adjust the mean BT for each of the three used channels. But ideally, we should be looking for a way to improve the classification.

Assuming that we wish to keep the principles of the existing AAPP test, one way to generate a new database (means and covariances) would be to use RadSim with the TELSEM version 2 land surface emissivity atlas (Prigent and Aires, 2016). This covers both land and sea-ice and uses a file for each month that includes emissivity information as well as a surface classification.

In total, TELSEM2 has 18 possible surface categories, with separate categories for land and sea-ice, but we could simplify this considerably for the purposes of AAPP, e.g. Table 2.

Table 2: A possible simplification of the TELSEM categories

	TELSEM category class 1	TELSEM category class2
Forest and dense vegetation	1-2	
Light vegetation	3-4	
Desert	5	
Snow and multi-year ice	6-9	
New ice	10	11-13
Wet land	10	10
Ocean	-	

		<h1>Adapting the AAPP microwave tests for EPS- SG</h1>	Doc ID :NWPSAF- MO-TR-040 Version : 1.0 Date : 23/05/2022
--	--	--	---

RadSim would need to be run for several different days (covering different seasons), with no cloud liquid water. Then geographical points would be selected that correspond to each surface category. The means and covariances of channels 1, 2 and 3 would be computed for each category.

The expectation is that the emissivity profiles of the different categories would be sufficiently different to allow them to be distinguished using the brightness temperatures. If this is not the case then the number of categories could be reduced further.

4.6 Bennartz test

In the Met Office, the “Bennartz” test is not run in AAPP, it is run in the Observation Processing System (OPS) prior to NWP assimilation. Over ocean, the scattering index is defined in OPS as:

$$SI = TB(89 \text{ GHz}) - TB(150 \text{ GHz}) - \text{offset (K)}$$

where $\text{offset} = a + b \text{ SatAng}$. A rain flag is triggered when $SI > \text{threshold}$, and the threshold used is 10K.

It appears that several different values have been used for the variable parameters a and b . A recent re-calibration has been done (S. Migliorini, pers. comm.) resulting in the following values:

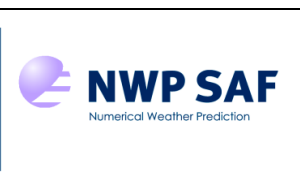
Operations: $TB_{\text{diff}} = -32.956 + 0.164 \text{ SZA}$
New linear fit: $TB_{\text{diff}} = -40.1775 + 0.2472 \text{ SZA}$

But note that OPS does not have access to the “*ave_back_sea*” (see section 2) that is used in AAPP (and originally coded by Ralf Bennartz), which should make the AAPP index more robust.

The Bennartz test uses 23.8 GHz only over land, therefore the MWS change of polarisation has no impact. MWS does, of course, use 166 GHz instead of 150 GHz, but this is already the case for ATMS. Therefore as a first implementation the test can be included unchanged for MWS.

4.7 Redundant tests

The “Grody light rainfall” and the “Crosby, Ferraro, Wu” tests are said to be “redundant” in the AAPP documentation, and therefore it is not proposed to carry these forward to MWS.

		<h1>Adapting the AAPP microwave tests for EPS- SG</h1>	Doc ID :NWPSAF- MO-TR-040 Version : 1.0 Date : 23/05/2022
--	--	--	---

5. CONCLUSIONS

The microwave tests in AAPP are useful for detecting cloud, precipitation and surface properties, in a way that is useful for applications such as pre-screening for NWP. It is desirable to implement at least some of these tests for MWS on EPS-SG.

MWS has some key differences in channel characteristics compared with AMSU and ATMS, notably the polarisation for the 23.8 GHz channel. This significantly changes the measured brightness temperature over ocean and needs to be considered when updating the microwave tests. MWS also has a new channel at 229 GHz, which provides new possibilities.

The following scattering tests are recommended for implementation in the AAPP pre-processor for MWS:

1. Scattering test (ocean): predict 89 GHz from 23.8, 31.4 and 50.3 GHz
2. Legacy cirrus test (ocean): predict 183 ± 7 GHz from 23.8, 89 and 166 GHz
3. New cirrus test (all surfaces): predict 229 GHz from 89, 166 and 183 ± 7 GHz
4. Surface test, using 23.8, 31.4 and 50.3 GHz
5. Bennartz rain test, using 23.8 (land only), 89 and 166 GHz

Tests 1 to 3 will benefit from new regression coefficients derived according to the methods outlined in section 4. But note that the actual values of the coefficients do not affect the software design.

Test 4 will require further effort in order to develop optimal coefficients, but a first iteration could be based on a slightly modified version of the coefficients used for AMSU and ATMS.

Test 5 can be unchanged from that implemented for AMSU and ATMS.

6. REFERENCES

- Bennartz, R., Thoss, A., Dybbroe, A. and Michelson, D.B. (2002), Precipitation analysis using the Advanced Microwave Sounding Unit in support of nowcasting applications. *Met. Apps*, 9: 177-189. <https://doi.org/10.1017/S1350482702002037>
- English S.J., R. J. Renshaw, P. C. Dibben, and J. R. Eyre, 1997: "The AAPP module for identifying precipitation, ice cloud, liquid water, and surface type on the AMSU-A grid". *Proceedings of the Ninth International TOVS Study Conference*, J. R. Eyre, Ed., ECMWF, 119–130 http://library.ssec.wisc.edu/research_Resources/publications/pdfs/ITSC9/english01_ITSC9_1997.pdf
- N. C. Grody, "Surface identification using satellite microwave radiometers" in *IEEE Transactions on Geoscience and Remote Sensing*, vol. 26, no. 6, pp. 850-859, Nov. 1988.
- Catherine Prigent and Filipe Aires, 2016: "Tool to Estimate Land Surface Emissivity at Microwaves and Millimeter waves", EUMETSAT Project EUM/CO/14/4600001473/CJA, available from <https://nwp-saf.eumetsat.int/site/software/rttov/download/> (included in TELSEM2 download).
- MWS Science Advisory Group, 2019: "EPS-SG MicroWave Sounder (MWS) Science Plan", available from https://www-cdn.eumetsat.int/files/2020-04/pdf_science_epssg_mws_plan.pdf